Biocompatible Anisole-Nonlinear PEG core-shell Nanogels for High Loading Capacity, Excellent Stability, and Controlled Release of Curcumin

Jing Shen , Jiangtao Zhang , Weitai Wu , Probal Banerjee , Shuiqin Zhou *

Posted Date: 30 August 2023

doi: 10.20944/preprints202308.1963.v1

Keywords: Core-shell nanogels; nonlinear PEG; anisole; biocompatible; thermo-responsive; curcumin stability, high loading capacity; drug delivery

Article

Biocompatible Anisole-Nonlinear PEG core-shell Nanogels for High Loading Capacity, Excellent Stability, and Controlled Release of Curcumin

Jing Shen [1,3], Jiangtao Zhang [1], Weitai Wu [2], Probal Banerjee [1] and Shuiqin Zhou [1,*]

[1] Department of Chemistry of The College of Staten Island, and The PhD Program in Chemistry of Graduate Center, The City University of New York, 2800 Victory Boulevard, Staten Island, NY 10314; jiangtao.zhang@cix.csi.cuny.edu (J.Z.); probalbanerjee@yahoo.com (P. B.)

[2] Department of Chemistry and The Key Laboratory for Chemical Biology of Fujian Province, College of Chemistry and Chemical Engineering, Xiamen University, Xiamen, Fujian 361005, China; wuwtxmu@xmu.edu.cn

[3] Department of Chemistry, Yunnan Normal University, Kunming 650092, China; shenjingbox0225@hotmail.com

* Correspondence: shuiqin.zhou@csi.cuny.edu

Abstract: Curcumin, a nontoxic and cheap natural medicine, has high therapeutic efficacy for many diseases including diabetes and cancers. Unfortunately, its exceedingly low water-solubility and rapid degradation in the body severely limit its bioavailability. In this work, we prepare a series of biocompatible poly(vinyl anisole)@nonlinear poly(ethylene glycol) (PVAS@PEG) core-shell nanogels with different PEG gel shell thickness to provide high water solubility, good stability, and controllable sustained release of curcumin. The PVAS nanogel core is designed to attract and store curcumin molecules for high drug loading capacity and the hydrophilic nonlinear PEG gel shell is designed to offer water dispersibility and thermo-responsive drug release. The obtained nanogels are monodispersed in spherical shape with clear core-shell morphology. The size and shell thickness of the nanogels can be easily controlled by changing the core-shell precursor feeding ratios. The optimized PVAS@PEG nanogels display a high curcumin loading capacity of 38.0 wt%. The nanogels can stabilize the curcumin from degradation at pH =7.4 and release the curcumin in response to heat in the physiologically important temperature range. The nanogels can enter cells effectively and exhibit negligible cytotoxicity to both the B16F10 and HL-7702 cells at a concentration up to 2.3 mg/mL. Such designed PVAS@PEG nanogels have a great potential to be used for delicate drug delivery.

Keywords: core-shell nanogels; nonlinear PEG; anisole; biocompatible; thermo-responsive; curcumin stability; high loading capacity; drug delivery

1. Introduction

Curcumin, a natural phenolic compound derived from the turmeric plants, has attracted a great deal of attention over the past decades due to its nontoxicity, low cost, and therapeutic effects for many diseases [1–3]. The ability to scavenge reactive oxygen radicals of curcumin molecules is believed to be the critical property for prevention and treatment of diseases. For example, the antioxidant property of curcumin can play an important role in diabetes therapy [4–14]. Unfortunately, the exceedingly low water-solubility and rapid metabolism in the body of curcumin severely limit its bioavailability [15–17]. In order to improve the bioavailability of curcumin, a variety of nanocarriers for curcumin have been developed [18–20], including polymer micelles [21–24], liposomes [25–28], inorganic nanoparticles [29–31], porous silica/metal-organic frames [32–34], biopolymer complexes/nanoparticles [35–39], and nanogels [40–49]. However, most of these

 doi:10.20944/preprints202308.1963.v1

nanocarriers developed so far exhibit low loading capacity or short circulation time, which still limited the bioavailability of curcumin for clinical use.

Responsive polymer nanogels offer great advantages for drug delivery due to their tunable size, favorable biocompatibility, an interior porous network structure for incorporation and protection of therapeutics, and controllable release by specific environmental stimuli [50–52]. The earliest polymer nanogel systems used to deliver curcumin is based on a copolymer nanogel (NanoCurcTM) from N-isopropylacrylamide, N-vinyl-2-pyrrolidone, and acrylic acid [43,44]. While curcumin loaded in this nanogel has remarkably higher systemic bioavailability than free curcumin in animal model, the therapeutic efficacy is still very limited due to the very low curcumin loading capacity (only 1.0-1.5 wt%) because of the hydrophilic nature of the nanogel. To introduce dual responsive curcumin delivery property, a variety of copolymer nanogels based on the thermosensitive poly(N-isopropylacrylamide) (pNIPAM) incorporated with pH-sensitive chitosan, poly(N,N-dimethylaminoethylmethacrylate) (pDMAEMA), and poly(allylamine) have been developed [46–48]. The incorporation of Au nanoparticles (NPs) into the polymer nanogels can induce a photothermal responsive release of curcumin [49,53]. The studies on these nanogels show that the design on the polymer materials of nanogels with specific affinity to the curcumin molecules is very important to improve the curcumin loading capacity. Our previous work shows that the increase of polystyrene domains in the nanogels can significantly enhance the curcumin loading capacity due to the hydrophobic nature of polystyrene [53]. Dinari et al. developed a dual responsive nanogels with the hyperbranched lignin NPs grafted with the crosslinked thermo-/pH- sensitive p(NIPAM-co-DMAEMA) copolymers, which show a high curcumin loading capacity because of the hydrophobic and hyperbranched nature of lignin [47]. However, the materials safety to biological systems of these nanogels composed of pNIPAM or polystyrene domains is still a big concern.

Poly(ethylene glycol) (PEG) is one of the few FDA approved polymers that can be used in biomedical fields due to its nontoxicity, non-immunogenicity, and biocompatibility. To combine the thermo-sensitivity, a group of nonlinear PEG derivatives have attracted great interest for bio-applications as an alternative to the pNIPAM [54–56]. More importantly, the lower critical solution temperature (LCST) of these nonlinear PEG polymers, polymerized from the oligo(ethylene glycol)-methacrylate macromonomers, can be precisely tuned into the range of physiologically interested temperature by varying the PEG side chain lengths [54–59]. These nonlinear PEG has been proved to be non-toxic and anti-immunogenic at relatively high concentration (100-250 μg/mL) by FDA standards [60]. On the other hand, anisole derivatives containing phenyl methyl ether moiety are natural ingredients produced by many conifers and herbs [61]. They are important intermediates in the synthesis of fragrances, pharmaceuticals, and a flavoring additive of bakery products [62]. Considering its structural similarity of the anisole moieties to the phenyl methyl ether units of curcumin molecules, we expect that curcumin molecules will have high affinity to the anisole moieties. Thus, a nanogel with polymer network chains composed of anisole moieties should enhance the curcumin loading capacity favorably.

In this work, we design a new type of responsive core-shell nanogels as drug nanocarriers with the aim to enhance both the curcumin loading capacity and the biocompatibility of polymers. Specifically, we synthesize an anisole-based nanogel core from the polymerization and crosslinking of 2-vinylanisole monomers (PVAS) followed by a deposition of the thermo-responsive nonlinear PEG gel shell (Scheme 1). The hydrophobic PVAS core is designed to attract and store curcumin molecules for high drug loading capacity and the biocompatible nonlinear PEG gel shell is designed to offer temperature responsive curcumin release. The synthetic approach for the core-shell nanogels based on stepwise precipitation polymerization in water is simple. The resultant PVAS@PEG nanogels are in spherical shape with clear core-shell morphology, narrow size distribution, controllable shell thickness, and thermo-responsive phase behavior. As expected, the PVAS@PEG nanogels display high curcumin loading capacity and thermo-controllable drug release in the physiologically important temperature range. Interestingly, the nonlinear PEG gel shell thickness can be used to tune the curcumin loading capacity and release kinetics. Our tests prove that the PVAS@PEG core-shell nanogels can stabilize the loaded curcumin molecules from degradation at the

physiological pH of 7.4. The MTT assay results show that the nanogels are nontoxic to both the mouse melanoma cells B16F10 and human hepatocyte cell HL-7702 at a concentration up to 2.3 mg/mL. The confocal imaging analysis indicates that the nanogels have good cell penetration ability. Such rationally designed PVAS@PEG core-shell nanogels should find wide applications for protection and delivery of other delicate hydrophobic therapeutic agents.

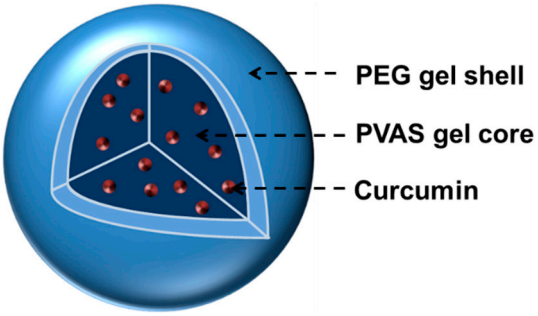

Scheme 1. Schematic illustration of curcumin-loaded core-shell nanogels with PVAS gel as a core and the nonlinear PEG gel as a shell. The hydrophobic curcumin drug is encapsulated within the inner PVAS core, which is coated by an outer PEG gel shell to offer both stability in aqueous media and temperature sensitivity.

2. Results and Discussion

2.1. Size and Morphology of the PVAS@PEG Core-Shell Nanogels

Our strategy to prepare the PVAS@PEG core-shell nanogels involves the first synthesis of a PVAS core nanogel followed by the deposition of the nonlinear PEG gel layer on the core template, based on the well-established precipitation polymerization method. The as-synthesized PVAS core nanogels made from the 2-vinylanisole monomers has a hydrodynamic radius (R_h) = 70 nm at 22 °C. This PVAS core was used as a template to prepare the nonlinear PEG gel shell polymerized from the comonomers of 2-(2-methoxyethoxy)ethyl methacrylate (M_n = 180 g/mol, MEO_2MA) and oligo(ethylene glycol) methyl ether methacrylate (M_n = 300 g/mol, MEO_5MA) and crosslinked by the PEG dimethacrylate (PEGDMA, $M_n \approx 550$ g/mol). In order to enable the resultant core-shell nanogel carriers to be responsive in the physiologically important temperature range, the molar ratio of the comonomers of MEO_2MA : MEO_5MA has been fixed at 1 : 2. Table 1 lists the size in terms of R_h measured at 22 °C of the resultant PVAS@PEG core-shell nanogels (coded as VEM) prepared from the different core-shell feeding compositions. The increase in the amount of the PEG shell precursors at a fixed amount of PVAS core nanogel particles in the synthetic mixtures gradually increases the overall size of the resultant PVAS@PEG nanogels. The R_h values of the core-shell nanogels of VEM1, VEM2, VEM3, and VEM4 are 101, 110, 138, and 165 nm, respectively. By subtracting the R_h (70 nm) of the PVAS core particles, the PEG gel shell thickness is 31, 40, 68, and 95 nm, respectively, for the VEM1, VEM2, VEM3, and VEM samples. This result indicates that the PEG gel shell thickness can be easily controlled by a simple change of the core-shell precursor feeding ratios in the synthesis.

Table 1. Feeding compositions and hydrodynamic radius (R_h) of the core-shell nanogels.

Sample	Core Solution (mmol)	Shell Solution (mmol)			R_h (nm)
	2-vinylanisole	MEO_2MA	MEO_5MA	PEGDMA	
PVAS core nanogel	0.594	—	—	—	70
PEG shell nanogel	—	0.75	1.50	2.26×10^{-2}	—
VEM1	0.594	0.20	0.40	0.60×10^{-2}	101
VEM2	0.594	0.25	0.50	0.75×10^{-2}	110
VEM3	0.594	0.50	1.00	1.51×10^{-2}	138
VEM4	0.594	0.75	1.50	2.26×10^{-2}	165

Preprints (www.preprints.org) | NOT PEER-REVIEWED | Posted: 30 August 2023 doi:10.20944/preprints202308.1963.v1

Figure 1 shows the size distributions of the PVAS@PEG core-shell nanogels, in terms of the R_h measured at T = 22 °C and θ = 45°, synthesized with different feeding amount of MEO_2MA and MEO_5MA comonomers but at the same molar ratio of 1:2. All the obtained nanogels have a very narrow size distribution. The dynamic light scattering (DLS) measurements indicate that the obtained nanogels are nearly monodispersed with a polydispersity index of $\mu_2/\langle\Gamma\rangle^2 = 0.001$.

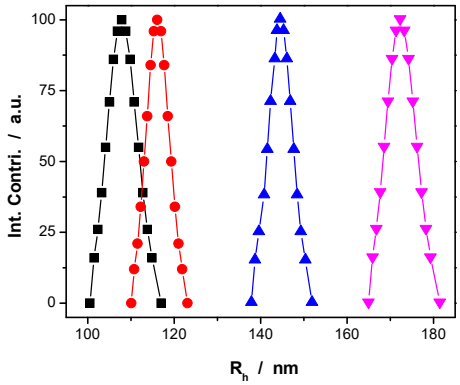

Figure 1. Hydrodynamic radius (R_h) distribution of the PVAS@PEG core-shell nanogels of VEM1 (■), VEM2 (●), VEM3 (▲), and VEM4 (▼), measured at 22 °C and a scattering angle of θ = 45°.

Figure 2 shows the typical TEM images of the dried core-shell nanogels of VEM2 and VEM3. Both nanogels exhibit a spherical shape and a well-defined core-shell architecture with a clear boundary between the dark condensed core and the light contrast shell. The dark core can be attributed to the high electron density of the PVAS chains crosslinked by the short crosslinker divinylbenzene (DVB). The oligo-PEG crosslinked nonlinear PEG gel shells have relatively low electron density and thus show lower contrast. The clear core-shell structure indicates that the densely crosslinked hydrophobic PVAS nanogel core can hinder the hydrophilic nonlinear PEG chains of the outer shell from interpenetrating into the inner core area. The TEM images also show that the shell of VEM3 nanogels is much thicker than that of the VEM2 nanogels although the nanogels are in dried state, further proving that the shell thickness of the core-shell nanogels can be tuned by simply adjusting the feeding ratio of the shell precursors to the PVAS core template in the synthesis.

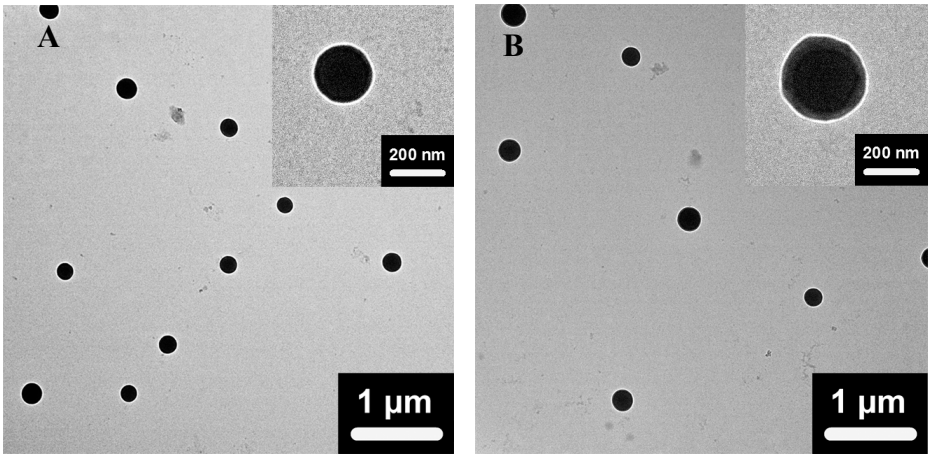

Figure 2. Typical TEM images of the core-shell structured PVAS@PEG nanogels VEM2 (A) and VEM3 (B).

2.2. Thermo-responsive volume phase transitions of the PVAS@PEG nanogels

Figure 3 shows the temperature-induced volume phase transitions of the PVAS@PEG core-shell nanogels in terms of the change of R_h values measured at a scattering angle of θ = 45°. Obviously, the

Preprints (www.preprints.org) | NOT PEER-REVIEWED | Posted: 30 August 2023 doi:10.20944/preprints202308.1963.v1

increase in temperature of the dispersion medium can induce a significant shrinkage of the core-shell nanogels. The hydrophobic PVAS core nanogels would not undergo conformational and chemical changes in water when giving external stimuli of temperature change. The observed temperature-induced volume phase transitions should be attributed to the thermosensitive nonlinear PEG gel shell. The nonlinear PEG network chains are composed of hydrophobic apolar carbon backbone grafted with hydrophilic PEG side chains. This counterbalance of the hydrophilic and hydrophobic forces results in the swelling/deswelling characteristic of the PEG gel shell. The critical volume phase transition temperature (VPTT) of the nonlinear PEG nanogels can be controlled by the feeding molar ratio of the two comonomers of MEO_2MA/MEO_5MA in synthesis [63]. As shown in Figure 3, the proper feeding molar ratio of the two macromonomers MEO_2MA/MEO_5MA = 1:2 in our PVAS@PEG nanogels produces a continuous shrinking in R_h values across the physiologically important temperature range of 37–42 °C, which are typical abnormal temperature range found in many pathological zones such as inflammation, diabetic wounds, and tumors. This temperature responsive volume phase transition of the nanogels is reproducible and reversible, which is important for the temperature responsive drug delivery. The results in Figure 3 also show that the nanogels do not reach a fully collapsed state at the experimental temperature window up to 50 °C, thus the nonlinear PEG gel shell is still partially swollen and hydrophilic at temperature below 50 °C, making the PVAS@PEG core-shell nanogel particles very stable in water. Even after few months, no sediment was observed in the nanogel solutions, which is critical to serve as a drug carrier for delivery of hydrophobic drugs. While the inner PVAS core provides hydrophobic region for the storage of hydrophobic drugs, the hydrophilic PEG gel shell can enable the nanogels to disperse in cell culture medium and further penetrate the cells. The thermo-responsive outer PEG gel shell can be utilized to regulate the transport of the drug molecules from the inner PVAS gel core region to the surrounding medium by temperature stimuli.

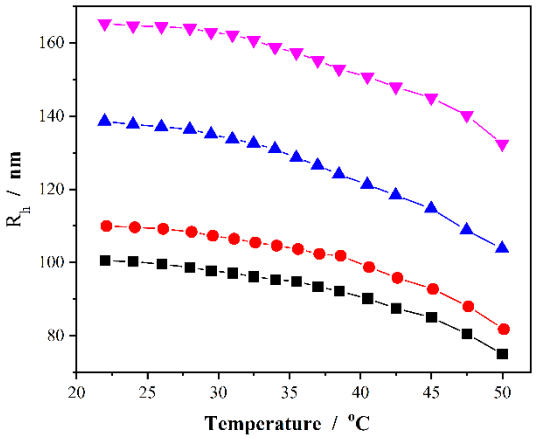

Figure 3. Temperature dependence of the average R_h values of the core-shell structured PVAS@PEG nanogels of VEM1 (■), VEM2 (●), VEM3 (▲), and VEM4 (▼), measured at a scattering angle θ = 45°.

2.3. Curcumin loading capacity of the PVAS@PEG nanogels

Curcumin is poorly soluble in water at acidic or neutral pH with the macroscopic un-dissolved flakes visible in the solution. On the other hand, curcumin molecules would undergo a rapid hydrolytic degradation and thus lose the pharmaceutical effects when pH is above the neutral value. It has been determined that the half-life time for the hydrolytic degradation of curcumin in aqueous solution containing 10% organic solvent at pH ≈ 6.0, 7.0, and 8.0 is 4.2 $\times 10^3$ h, 15 h and 3.5 $\times 10^{-2}$ h, respectively. Therefore, we loaded the curcumin molecules into the PVAS@PEG core-shell nanogels at pH = 5.7, where the curcumin molecules should have no significant degradation occurred. From our experiences, two factors can determine the drug loading capacity for nanogel based drug carriers. One is the affinity of the drug molecules to the polymer network chains in the gel. Another is the storage space of the nanogels for the drug molecules. In our design of the PVAS@PEG core-shell

 doi:10.20944/preprints202308.1963.v1

nanogels, the anisole units of the PVAS core nanogels have a similar structure to the phenyl methyl ether units in the curcumin molecules, thus the drug affinity to the PVAS network chains in the core should be very high through the π-π stacking and other association interactions, which is important to attract the curcumin molecules into the core region. However, the hydrophobic PVAS core nanogels crosslinked by small DVB molecules are in collapsed state in aqueous phase. To open the PVAS network of the core nanogels, the hydrophilic PEG gel shell takes important role. We expect that the swelling of the hydrophilic PEG gel shell will pull up the PVAS network chains in the core and thus open the pores of the PVAS core nanogels for storage of the hydrophobic curcumin molecules.

Figure 4 shows the effect of the PEG gel shell thickness on the drug loading capacity of the PVAS@PEG core-shell nanogels measured at 22 °C. The curcumin loading capacity was determined to be 18.5 wt%, 29.3 wt%, 31.9 wt%, 35.5 wt%, and 38.0 wt% for the PVAS core, VEM1, VEM2, VEM3, and VEM4 nanogels, respectively. Clearly, the addition of the hydrophilic nonlinear PEG gel shell onto the PVAS core can significantly enhance the curcumin loading capacity. The thicker the nonlinear PEG gel shell, the higher the drug loading capacity of the core-shell nanogels. Interestingly, the influence of the PEG gel shell thickness on the curcumin loading capacity has a transition point around 40 nm. When the gel shell thickness is below 40 nm, the addition of the PEG shell onto the core induces a much larger increase in the drug loading capacity. The further increase in the thickness of the PEG gel shell continuously increases the curcumin loading capacity but at a much smaller pace. This result implies that the hydrophilic PEG gel shell has limited ability to attract the hydrophobic curcumin drug molecules. Indeed, this was confirmed by the extremely low curcumin loading capacity of 1.52 wt% for the nonlinear PEG nanogels with the same composition as the nonlinear PEG gel shell in the core-shell nanogels (See Table 1). In contrast, the PVAS core alone demonstrates a much higher curcumin loading capacity (18.5 wt%) than these nonlinear PEG nanogels, because of the good affinity of the curcumin to the PVAS core network chains. This result supports that the curcumin drug molecules are mainly stored in the hydrophobic PVAS nanogel core region. Then the question becomes why the addition of the hydrophilic PEG gel shell can further significantly enhance the curcumin loading capacity of the core-shell nanogels. To answer this question, we need consider the influence from the pore size of the core nanogel network besides the drug affinity to the nanogel matrix. Without the hydrophilic PEG gel shell, the hydrophobic PVAS core is in a collapsed state with small mesh size of the PVAS chain network, which has limited space to host the curcumin drug molecules. After introducing the hydrophilic nonlinear PEG gel shell, the swollen gel shell can pull up and stretch the PVAS core network chains, and thus enlarge the mesh size of PVAS core network although the core network chains are still hydrophobic. The open network with large mesh size of the hydrophobic PVAS core could host much more hydrophobic curcumin molecules. The thicker the swollen nonlinear PEG gel shell, the larger the pulling force to open the hydrophobic PVAS core network, resulting in higher curcumin loading capacity of the core-shell nanogels. When the shell thickness is increased to a certain value, the mesh size of the hydrophobic PVAS core network chains will no longer increase due to the limitation of chemical crosslinking. As such, the drug loading capacity of the core will also reach a maximum value. That's why the further increase in the thickness of PEG gel shell larger than 40 nm would only increase the curcumin loading capacity slightly for the PVAS@PEG core-shell nanogels, because the PEG gel shell alone has very low loading capacity for hydrophobic curcumin molecules.

Preprints (www.preprints.org) | NOT PEER-REVIEWED | Posted: 30 August 2023 doi:10.20944/preprints202308.1963.v1

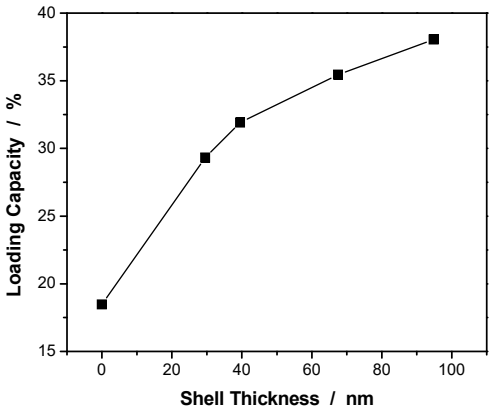

Figure 4. Curcumin loading capacity of the PVAS@PEG core-shell nanogels as a function of the nonlinear PEG gel shell thickness, measured at 22 °C.

2.4. Curcumin stability in the PVAS@PEG nanogels

The hydrolytic degradation of curcumin molecules occurs rapidly in aqueous phase when the pH is above neutral value [64]. Wang et al. have used high performance liquid chromatography and mass spectrometry to monitor the degradation of curcumin molecules. The results show that curcumin molecule is partially deprotonated initially, followed by fragmentation into trans-6-(4-hydroxy-3-methoxyphenyl)-2,4-dioxo-5-hexanal as the main product, then further decomposed to vanillin, ferulic acid, and feruloyl methane [65]. The degradation of curcumin molecules can also be monitored by photospectroscopic technique because the degraded products of curcumin contribute very little to the optical emission signal [66].

Figure 5 compares the fluorescence intensity change of the free curcumin molecules (A) and the curcumin molecules loaded into the PVAS@PEG core-shell nanogels (sample VEM3) (B) dispersed in a PBS solution at pH = 7.4, with the photoluminescence (PL) spectra recorded over 180 min at 37 °C and 15 min intervals. The results show that the PL intensity of the free curcumin molecules obtained at an excitation wavelength (λex) = 420 nm in PBS of pH = 7.4 at 37 °C decreases rapidly with ~ 65% of curcumin molecules degraded over the 3 h course. In contrast, the PL intensity of the curcumin molecules loaded in the PVAS@PEG nanogels still remains strong with only ~ 10% of curcumin molecules degraded over the initial 45 min and only about 5% of curcumin degraded over the remaining 2.5 h (Figure 5C). The initial fast degradation rate, similar to that of free curcumin molecules under the same conditions, could be attributed to those curcumin molecules adsorbed on the surface layer of the nanogels. Obviously, the curcumin molecules loaded in the inner core of the PVAS@PEG nanogels are very stable against degradation at pH = 7.4 and 37 °C, which proves that nanogel drug carriers can protect the delicate drug molecules from degradation.

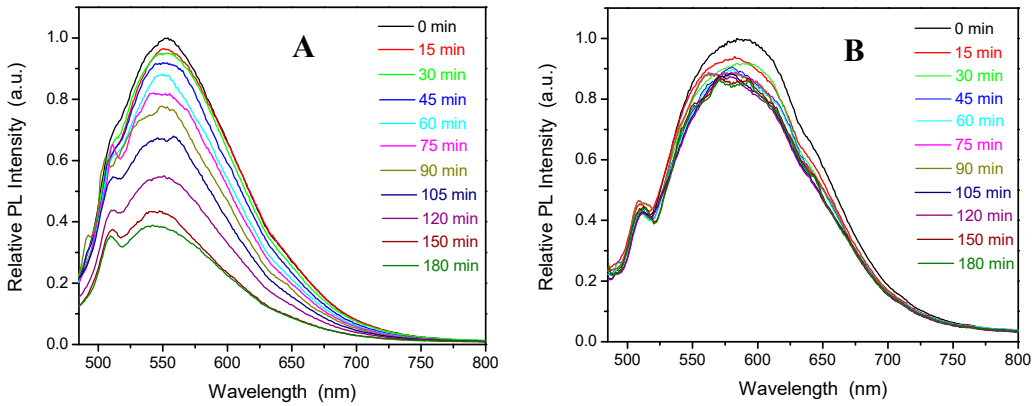

Preprints (www.preprints.org) | NOT PEER-REVIEWED | Posted: 30 August 2023 doi:10.20944/preprints202308.1963.v1

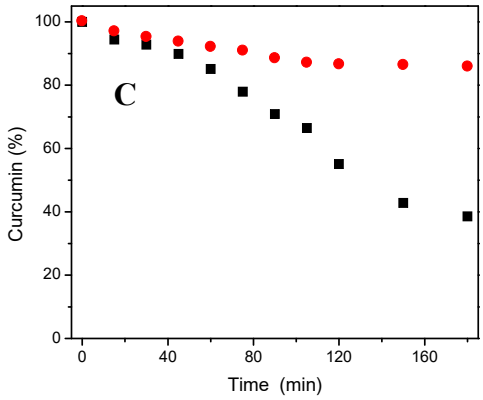

Figure 5. Fluorescence spectra of the free curcumin molecules (A) and curcumin-loaded PVAS@PEG (VEM3) nanogels (B) in a pH = 7.4 PBS buffer solution over a course of 180 min. The decays of the emitted fluorescence intensity at the maxima are shown in C (●: curcumin-loaded VEM3, ■: free curcumin). All experiments were carried out at 37 °C.

2.5. Thermo-responsive curcumin release from the PVAS@PEG nanogels

Figure 6 shows the release kinetics of curcumin molecules from the PVAS@PEG core-shell nanogels of sample VEM1, VEM2, VEM3, and VEM4, respectively, at different temperatures. The in vitro release tests were carried out in a PBS of pH = 6.15 to avoid the evident degradation of curcumin from the long-time exposure in water. A blank release experiment of free curcumin solution (containing ~5% ethanol) with an equivalent amount of drug to that loaded in the VEM1 nanogel was also performed, showing that the dialysis membrane (cutoff 12000 – 14000 Da) played a negligible role in the release kinetics (Figure 6A). Three features should be noted. Firstly, the curcumin release from the core-shell nanogels is much slower than from the free curcumin solution, indicating a sustained release of curcumin from the core-shell nanogel carriers. Secondly, the release kinetics of curcumin from the core-shell nanogels is thermo-responsive. The release of curcumin could be significantly speeded up by increasing temperature for all the VEM1, VEM2, VEM3 and VEM4 core-shell nanogels. For instance, only 16.1% of curcumin was released from VEM1 at 22 °C after 72 h. When temperature of the dispersing medium was increased to 37, 39, and 41 °C, the percentage of curcumin released from VEM1 reached to 44.4%, 65.3%, and 80.4% after the same period (72 h). This temperature dependence of curcumin release should be attributed to the thermo-responsive nonlinear PEG gel shell. The increase in temperature induced a gradual shrinking of the PEG gel shell and thus reduced the pulling force for the hydrophobic core, which in turn compressed the core space and thus squashed out the curcumin molecules. Meanwhile, the PEG gel shell shrunk at the raised temperatures and the thinner shell thickness could also reduce the restricted diffusion path length of curcumin molecules from the core region to the medium outside of the nanogels. The higher the temperature of the releasing medium, the thinner the PEG gel shell, which compressed more on the PVAS core, thus more curcumin molecules could be released from the core-shell nanogels. Thirdly, a slightly quicker release rate was determined at all the investigated temperatures for the PVAS@PEG core-shell nanogels with thinner PEG gel shell. For example, the percentage of curcumin released from VEM1, VEM2, VEM3 and VEM4 at 41 °C over 72 h is 80.4%, 78.0 %, 75.9%, and 73.7%, correspondingly. This result could also be attributed to the factor that the thin gel shell can shorten the restricted diffusion path of the curcumin molecules from the core region to the external dispersion medium of the nanogel particles.

Preprints (www.preprints.org) | NOT PEER-REVIEWED | Posted: 30 August 2023 doi:10.20944/preprints202308.1963.v1

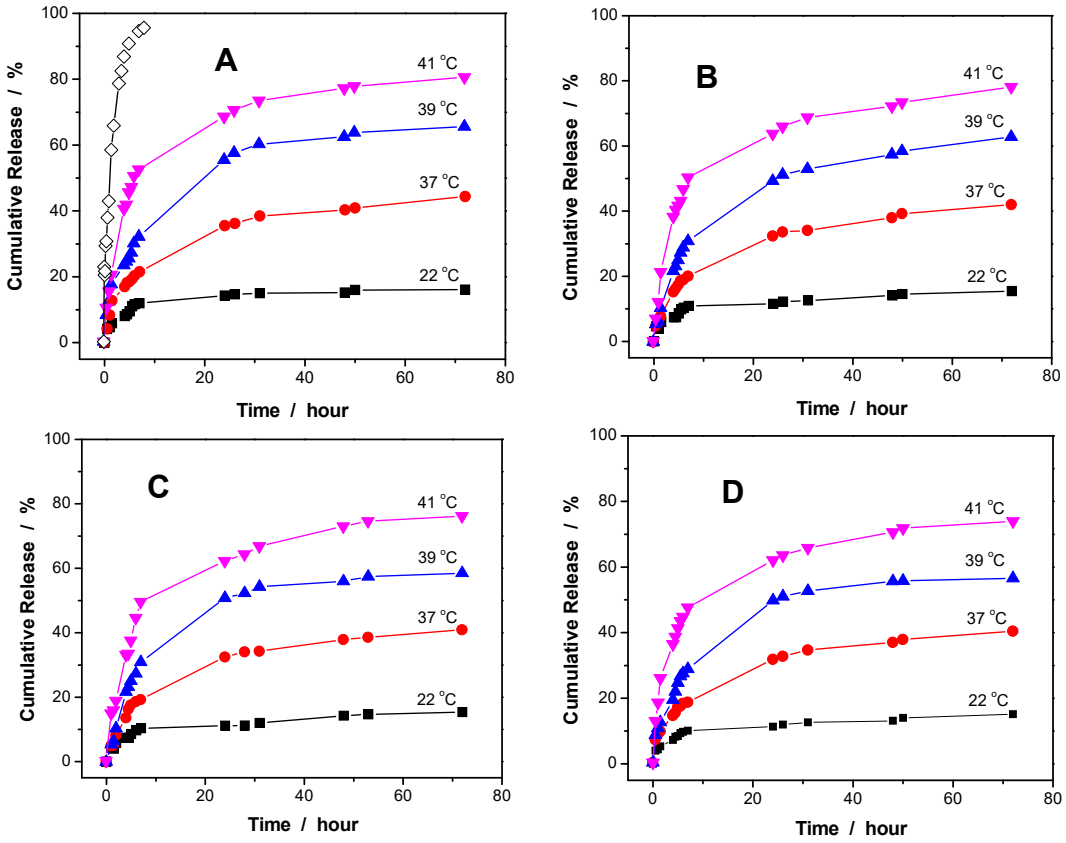

Figure 6. Releasing profiles of the curcumin molecules (preloaded at 22 °C) from the PVAS@PEG core-shell nanogels of VEM1 (A), VEM2 (B), VEM3 (C), and VEM4 (D) at different temperatures. In the blank (◊), 1 mL diluted solution of free curcumin (containing 5% ethanol) with an equivalent amount of drug trapped in the VEM1 sample was performed at 41 °C. All releasing experiments were carried out in 50 mL PBS (0.005M) of pH = 6.15.

2.6. Cellular Internalization of the PVAS@PEG nanogels

To test the cellular internalization ability of drug carriers, laser confocal imaging on cells is a good technique if the nanocarriers can display strong fluorescence or tagged with fluorescent objects. In our system, the free PVAS@PEG nanogels do not emit significant fluorescence in the available wavelength range of the confocal imaging equipment. On the other hand, curcumin molecules can emit strong visible fluorescence under the physiological conditions. Therefore, if we load the curcumin molecules into the PVAS@PEG nanogels, the fluorescent curcumin stabilized in the core region of the nanogels should enable us to detect whether the nanogels enter into the cells by using laser confocal imaging. However, one challenge is to prevent the free curcumin molecules mixed with the curcumin-loaded nanogels when the cells are incubated with nanogels in the culture medium at 37 °C, because free curcumin molecules can enter the cells and illuminate the cells as well when excited by laser. To solve this issue, we loaded the curcumin to the PVAS@PEG core-shell nanogels at 37 °C and allow the release of curcumin molecules from the peripheral region of the nanogels for 7 days at 37 °C. As shown in Figure 7, when the curcumin molecules were loaded into the nanogels at 37 °C, only 15.6% and 12.9% of loaded curcumin was released over 72 h at 37 °C from the VEM2 and VEM3 nanogels, respectively. Moreover, the curcumin release mainly occurs in the first 10 h (should be from the peripheral region). After 48 h, the curcumin release is negligible. Therefore, the procedure of loading curcumin at 37 °C followed by 72 h release can ensure no free curcumin molecules further released from the core-shell nanogels when cells are incubated with these curcumin-loaded nanogels in culture medium at 37 °C. As such, only curcumin molecules still retaining in the core region of nanogels can emit fluorescence for cellular imaging.

Preprints (www.preprints.org) | NOT PEER-REVIEWED | Posted: 30 August 2023 doi:10.20944/preprints202308.1963.v1

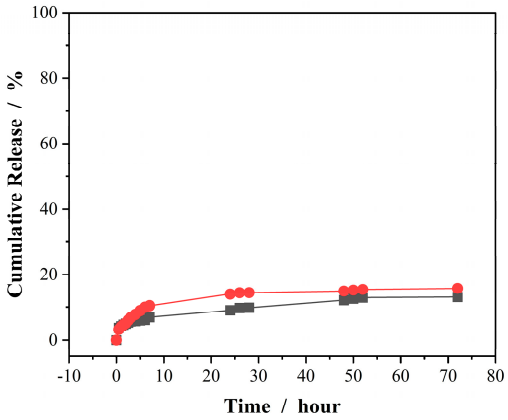

Figure 7. Releasing profiles of curcumin molecules from the PVAS@PEG nanogels of VEM2 (●) and VEM3 (■) at 37 °C. The curcumin molecules are pre-loaded into the nanogels at 37 °C. All releasing experiments were carried out in 50 mL PBS (0.005M) of pH = 6.15.

Figure 8 shows the scanning confocal fluorescence images of the mouse melanoma cells B16F10 after incubated with the curcumin-loaded PVAS@PEG core-shell nanogels (processed by 72h release) for 2 h, irradiated by a laser with the wavelength of 496 nm. The bright fluorescence observed on the cells should be attributed to the curcumin molecules encapsulated inside the core-shell nanogels, because these curcumin molecules in the core region are stable with no degradation (See Figure 5). In contrast, free curcumin molecules would have degraded by ~50% over the 2 h incubation if they were present. No significant autofluorescence of cells was observed under similar conditions. To confirm that the nanogels are not just attached on the surface of cells, the top-down Z-scanning confocal fluorescence images were taken for the B16F10 cells (Figure 9), which indicate that the curcumin-loaded PVAS@PEG core-shell nanogels indeed enter the cells and illuminate the entire cell. All the four nanogels with different PEG gel shell thickness can overcome cellular barriers and penetrate into the B16F10 cells successfully. The nanogels are mainly distributed in the cytoplasm and perinuclear region of the cells. The mechanisms of endocytosis of nanoparticles should be viewed in a broader context than simple vesicular trafficking. For our PVAS@PEG nanogels, the endocytosis process might be associated with the small size and specific surface properties. These results reveal that the designed PVAS@PEG core-shell nanogels can be used for intracellular drug delivery.

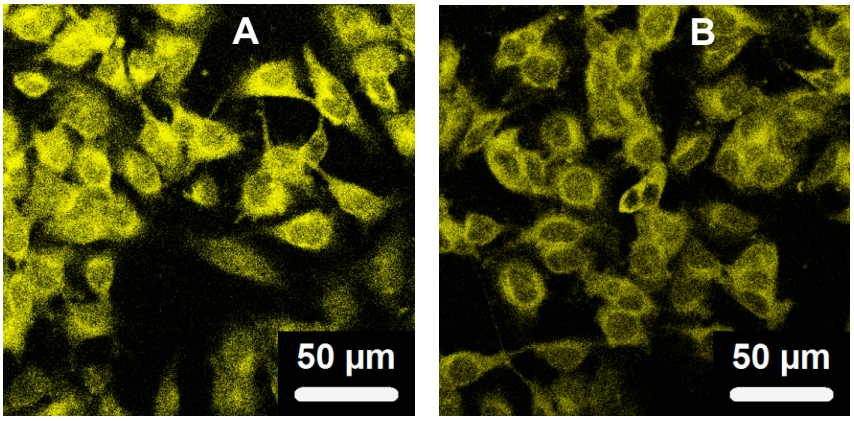

Preprints (www.preprints.org) | NOT PEER-REVIEWED | Posted: 30 August 2023 doi:10.20944/preprints202308.1963.v1

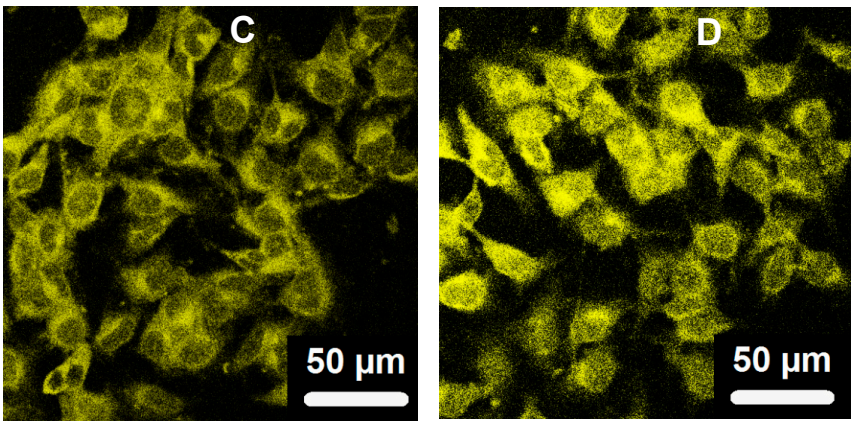

Figure 8. Scanning confocal fluorescence images of mouse melanoma B16F10 cells incubated with with the curcumin-loaded PVAS@PEG nanogels: VEM1 (A), VEM2 (B), VEM3(C), and VEM4 (D), respectively. Excitation wavelength is 496 nm.

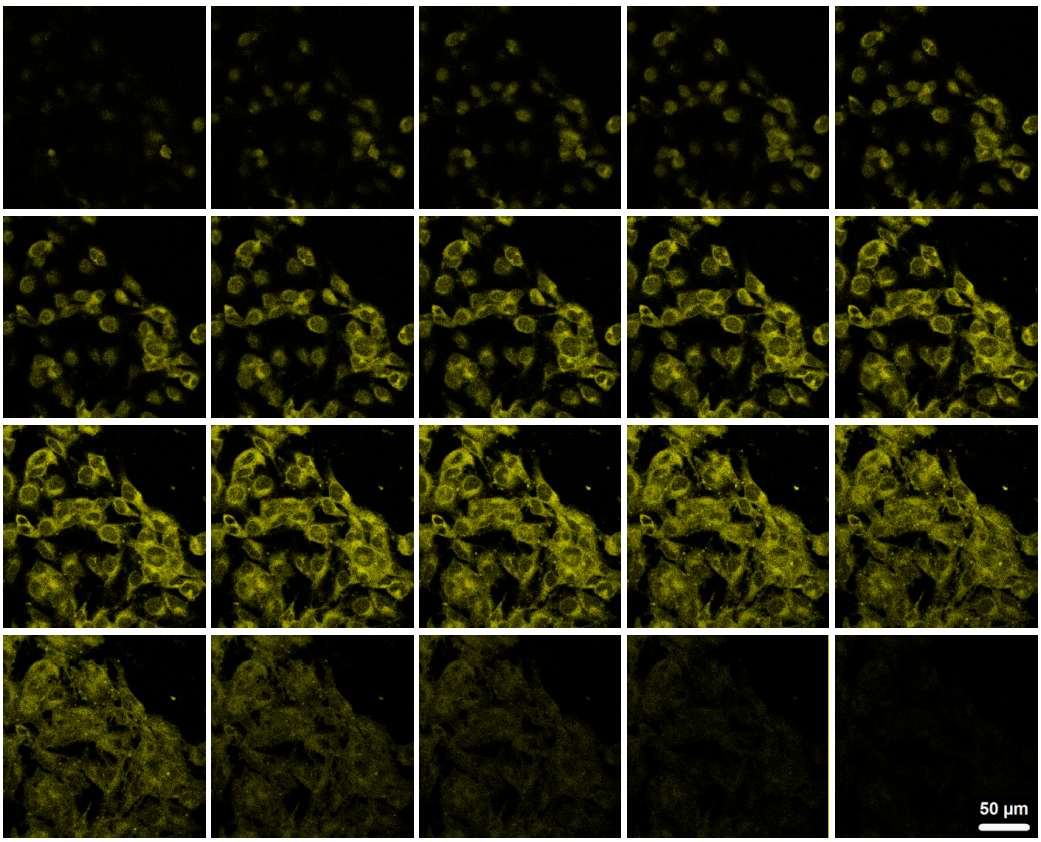

Figure 9. Z-Scanning confocal fluorescence transmission images of mouse melanoma cells B16F10 incubated with the curcumin-loaded PVAS@PEG core-shell nanogels (VEM3).

2.7. In vitro cytocompatibility of the PVAS@PEG nanogels

For biological applications, the safety of the drug carrier materials is critical. To test the cytotoxicity of the PVAS@PEG core-shell nanogels, two cell lines of the mouse melanoma B16F10 cells and the human hepatocyte HL-7702 cells were selected for exposure to the core-shell nanogels at different concentrations. As one of the most important human cell lines, human hepatocyte cells play indispensable role in metabolism, such as bile production and detoxication. The cell viability was quantified by MTT assay. Figure 10 shows the cell viability of the B16F10 cells (A) and HL-7702 cells (B), respectively, upon treatment with the PVAS@PEG nanogels of VEM1 sample at different concentrations. Both the B16F10 cells and HL-7720 cells continue growing in the cell culture medium containing the PVAS@PEG nanogels at concentrations up to 2300 μg/mL with viability over 100%

Preprints (www.preprints.org) | NOT PEER-REVIEWED | Posted: 30 August 2023 doi:10.20944/preprints202308.1963.v1

after 24 h incubation. These results indicate that the PVAS@PEG core-shell nanogels have negligible cytotoxicity against both tumor cells and normal cells. Such good biocompatibility of the newly designed nanogels is crucial for drug delivery applications, because the cells can tolerate very high concentrations of the drug carriers to deliver high dose of drug molecules in a sustained and intelligent releasing manner.

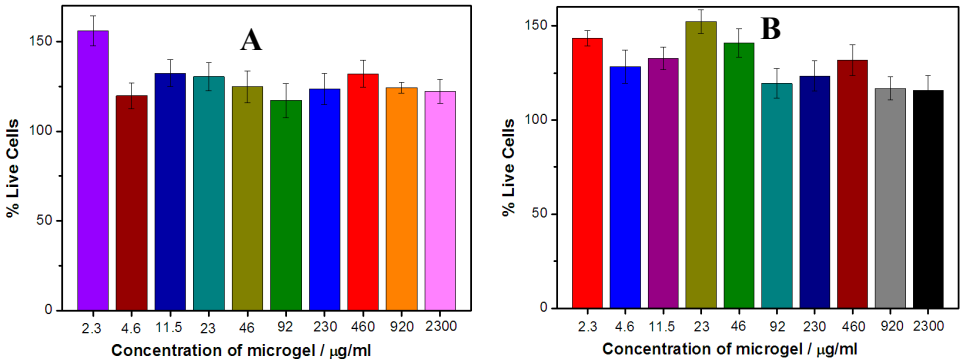

Figure 10. In vitro cytotoxicity results of PVAS@PEG nanogels VEM1 at different concentrations against the mouse melanoma cells B16F10 (A) and the human hepatocyte cell HL-7702 (B), respectively.

3. Conclusion

Well-defined thermo-responsive PVAS@PEG core-shell nanogels with the anisole-based PVAS nanogel as the hydrophobic core and the temperature-sensitive nonlinear PEG gel as a hydrophilic shell could be successfully synthesized via precipitation polymerization. Both the drug-carrier affinity and the pore (or mesh) size of the core-shell nanogels are important to enhance the drug loading capacity. The rationally designed PVAS core chains can effectively attract, store, and protect the delicate hydrophobic curcumin molecules via π-π stacking and other association interactions, providing high drug loading capacity and stability. The hydrophilic nonlinear PEG gel shell cannot only enable the resultant core-shell nanogels dispersed very well in aqueous media, but also pull up the hydrophobic PVAS core network chains (increase the mesh size) to further enhance the loading capacity by increasing the PEG shell thickness. The sustained release of the preloaded curcumin molecules from the core-shell nanogels can be triggered by local heat in the physiologically important temperature range. The PVAS@PEG core-shell nanogels can easily penetrate into cells. The nanogel carriers have negligible cytotoxicity against both tumor cells and normal cells in the tested concentration range up to 2.3 mg/mL, providing the ability to carry high dose of drug molecules and then release them intelligently in a sustained manner. The core-shell nanogels can be extended to load other delicate hydrophobic drugs and should find wide applications in drug delivery field.

4. Materials and Methods

4.1. Materials

2-(2-methoxyethoxy)ethyl methacrylate (MEO_2MA, 95%), oligo(ethylene glycol)methyl ether methacrylate (MEO_5MA, Mn = 300 g/mol), poly(ethylene glycol) dimethacrylate (PEGDMA, Mn ≈ 550 g/mol), 2-vinylanisole, divinylbenzene (DVB), 2,2′-azobis(2-methylpropionamidine) dihydrochloride (AAPH), sodium dodecyl sulfate (SDS), curcumin, anhydrous ethanol, Dulbecco's Modified Eagle Medium (DMEM), and Fetal bovine serum (FBS) were purchased from Sigma Aldrich. MEO_2MA, MEO_5MA and PEGDMA were purified with neutral Al_2O_3. Curcumin was purified with anhydrous ethanol. The water used in all experiments was of Millipore Milli-Q grade.

 doi:10.20944/preprints202308.1963.v1

4.2. Synthesis of PVAS core nanogels

The core nanogels were prepared by free radical precipitation copolymerization of 2-vinylanisole using AAPH as an initiator. A mixture of 2-vinylanisole (5.96×10^{-4} mol), DVB (5.61×10^{-5} mol), SDS (3.46×10^{-4} mol), and water (95 mL) was poured into a 250 mL three-neck round-bottom flask equipped with a stirrer, a nitrogen gas inlet, and a condenser. After 30 min, the temperature was raised to 70 °C and the polymerization was initiated by adding 1 mL of AAPH (0.105 M). The polymerization was allowed to proceed for 5 h. The resulted solution was centrifuged three times at 10,000 rpm (30 min, Thermo Electron Co. SORVALL® RC-6 PLUS superspeed centrifuge) with supernatant discarded and the precipitate redispersed in 200 mL deionized water. The resultant PVAS nanogels were used as core template for subsequent precipitation polymerization to add the nonlinear PEG gel shell.

4.3. Synthesis of PVAS@PEG core-shell nanogels

The nonlinear PEG shell precursors of MEO_2MA and MEO_5MA comonomers mixture in 1:2 molar ratio and PEGDMA crosslinker were dissolved into the 100 mL purified PVAS core nanogel dispersion. The mixture was heated to 70 °C under a N_2 purge. After 30 min, 1 mL of AAPH (0.105 M) initiator was added to start the polymerization. The synthesis was allowed to proceed to total 5 h. The resulted PVAS@PEG core-shell nanogels were purified with centrifugation/redispersion in water for three cycles, followed by 3 days of dialysis (Spectra/Pro® molecularporous membrane tubing, cutoff 12,000–14,000) against very frequently changed water at room temperature (~22 °C). Different feeding compositions of the core nanogels and the PEG gel shell precursors were used to control the nonlinear PEG gel shell thickness.

4.4. Curcumin loading and release

Loading: 5 mL of nanogel dispersion was stirred in an ice water bath for 30 min. 4 mL fresh curcumin solution of 1mg/mL in anhydrous ethanol was then added dropwise to the vial. After stirring overnight, the suspension was centrifuged at 10,000 rpm for 15 min at 22 °C. To remove free curcumin, the precipitate was redispersed in 5 mL water, and further purified by repeated centrifugation and washing at least six times. All the upper clear solutions were collected, and the concentration of free curcumin solution was determined by fluorescence spectrophotometer at 566 nm upon excitation at 420 nm. Optical signal was converted to concentration based on the linear calibration curve $R^2 > 0.99$ measured using the standard solutions of curcumin under the same condition. The amount of loaded curcumin in the nanogels was calculated by deducting the amount of curcumin in upper clear solution from the total curcumin amount (4 mg). The loading capacity is expressed as the mass of loaded drug per unit weight of dried nanogels. The loading experiments at physiological temperature 37 °C were also performed by using the same procedure as that at 22 °C.

The in vitro release of curcumin from the nanogels was evaluated by the dialysis method. The curcumin-loaded nanogel dispersion was diluted to 0.15 mg/mL for the release experiments. A dialysis bag (Spectra/Pro® molecularporous membrane tubing, cutoff 12,000–14,000) filled with 1 mL diluted curcumin-loaded nanogels was immersed in 50 mL 0.005 M phosphate buffer solutions (PBS) of pH = 6.15 at different temperatures. The released curcumin outside of the dialysis bag was sampled at a defined period and assayed by fluorescence spectrophotometer at 566 nm upon excitation at 420 nm. Cumulative release is expressed as the total percentage of drug released through the dialysis membrane over time.

4.5. Internalization of nanogels into mouse melanoma cells B16F10

Round glass coverslips were placed in wells of a 24-well plate and treated with 0.1% poly-L-lysine in 100 mM PBS for 40 min. Following the treatment, the solution was aspirated and the wells were washed with PBS 3 times each. Next, B16F10 cells were plated on the glass coverslips at 80% confluence in DMEM containing 10% FBS and 1% penicillin-streptomycin. After 24 h, 500 µL of the four curcumin-loaded nanogels (0.3 µg/mL) with different PEG gel shel thickness in serum-free

Preprints (www.preprints.org) | NOT PEER-REVIEWED | Posted: 30 August 2023 doi:10.20944/preprints202308.1963.v1

DMEM were added into the wells respectively. The plate was incubated at 37 °C for 2 h. The medium was then aspirated and fresh serum-free DMEM was added to each well. Finally, the coverslips with cells were removed from the wells and mounted onto slides for confocal microscopy study.

4.6. In vitro cytotoxicity

B16F10 cells and Human hepatocyte HL-7702 cells (both 6 × 10^3 cells/well) were cultured in DMEM containing 10% FBS and 1% penicillin-streptomycin in a 96-well plate and exposed to different concentration of PVA@PEG core-shell nanogels, respectively. The plate was washed three times using fresh serum-free DMEM. The plate was incubated at 37 °C for 24 h. After that, 25 μL of 3-(4,5-dimethyl-2-thiazolyl)- 2,5-diphenyltetrazolium bromide (MTT) solution (5 mg/mL in phosphate buffered saline (PBS)) were added to the wells. After incubation for 2 h, the solution was aspirated and 100 μL of DMSO was added to each well to dissolve the formazan crystal, and the plate was sealed and incubated overnight at 37 °C with gentle mixing. Three portions of the solution obtained from each well were transferred to the three respective wells of a 96-well plate. Cell viability was measured using a microplate reader at 570 nm. Positive controls contained no nanogels, and negative controls contained MTT.

4.7. Characterization

The TEM images were taken on a FEI TECNAI transmission electron microscope at an accelerating voltage of 120 kV. Approximately 10 μL of diluted nanogel suspension was dropped on a Formvar covered copper grid (300 meshes) and then air-dried at room temperature for the TEM measurements. The fluorescence spectra (or PL spectra) were respectively obtained on a JOBIN YVON Co.FluoroMax®-3 Spectrofluorometer equipped with a Hamamatsu R928P photomultiplier tube, calibrated photodiode for excitation reference correction from 200 to 980 nm, and an integration time of 1 s. The pH values were obtained on a METTLER TOLEDO SevenEasy pH meter. The B16F10 cells incorporated with nanogels were imaged using a confocal laser scanning microscopy (LEICA TCS SP2 AOBSTM) equipped with an HC PL APO CS 20 × 0.7 DRY len. The DLS measurements were performed on a standard laser light scattering spectrometer (BI-200SM) equipped with a BI-9000 AT digital time correlator (Brookhaven Instruments, Inc.). A Nd:YAG laser (150 mW, 532 nm) was used as the light source. All nanogel solutions were passed through Millipore Millex-HV filter with a pore size of 0.80 μm to remove dust before the DLS measurements. In DLS, the Laplace inversion of each measured intensity-intensity time correlated function can result in a characteristic line width distribution G(Γ). For a purely dissuasive relaxation, Γ is related to the translational diffusion coefficient D by $(\Gamma/q^2)_{C\to 0,q\to 0} = D$, where $q = (4\pi n/\lambda)\sin(\theta/2)$ with n, λ, and θ being the solvent refractive index, the wavelength of the incident light in vacuo, and the scattering angle, respectively. G(Γ) can be further converted to a R_h distribution by using the Stokes-Einstein equation, $R_h = (k_B T)/(6\pi\eta D)$, where k_B, T, and η are the Boltzmann constant, the absolute temperature, and the solvent viscosity, respectively.

Author Contributions: Conceptualization and methodology design, W. W. and S. Z.; synthesis and characterization, J. S. and J. Z.; cell imaging: J. S. and P. B.; cell viability: J. S. and W. W.; Data analysis, interpretation, writing, review, and editing, J.S., J. Z., W. W., and S. Z.; supervision, project administration, funding acquisition, S. Z. All authors have read and agreed to the published version of the manuscript.

Funding: This research was funded by NIH-NIDDK with grant number 1R15DK127360-01A1. J.S. was partially supported by Yunnan Provincial Science and Technology Department 202301AT070071.

Institutional Review Board Statement: Not applicable.

Informed Consent Statement: Not applicable.

Data Availability Statement: Not applicable.

Conflicts of Interest: The authors declare no conflict of interest.

References

1. Salehi, B.; Stojanovic-Radic, Z.; Matejic, J.; Sharifi-Rad, M.; Kumar, N. V. A.; Martins, N.; Sharifi-Rad, J. The therapeutic potential of curcumin: A review of clinical trials. *Eur. J. Med. Chem.* **2019**, *163*, 527−545.
2. Kunnumakkara, A. B.; Hegde, M.; Parama, D.; Girisa, S.; Kumar, A.; Daimary, U. D.; Garodia, P.; Yenisetti, S. C.; Oommen, O. V.; Aggarwal, B. B. Role of Turmeric and Curcumin in Prevention and Treatment of Chronic Diseases: Lessons Learned from Clinical Trials. *ACS. Pharmacol. Transl. Sci.* **2023**, *6*, 447−518.
3. Karthikeyan, A.; Senthil, N.; Min, T. Nanocurcumin: A Promising Candidate for Therapeutic Applications. *Front. Pharmacol*. **2020**, *11*, 487.
4. Salehi, B.; Quispe, C.; Chamkhi, I.; Omari, N. E.; Balahbib, A.; Sharifi-Rad, J.; Bouyahya, A.; Akram, M.; Iqbal, M.; Docea, A. O.; Caruntu, C.; Leyva-Gomez, G.; Dey, A.; Martorell, M.; Calina, D.; Lopez, V.; Les, F. Pharmacological Properties of Chalcones: A Review of Preclinical Including Molecular Mechanisms and Clinical Evidence. *Front. Pharmacol*. **2021**, *11*, article 592654.
5. Zhang, D.; Fu, M.; Gao, S.; Liu, J. Curcumin and Diabetes: A Systematic Review. *Evid. Based. Complement. Alternat. Med.* **2013**, 636053.
6. Marton, L. T.; Pescinini-E-Salzedas, L. M.; Camargo, M. E. C.; Barbalho, S. M.; Haber, J. F. D. S.; Sinatora, R. V.; Detregiachi, C. R. P.; Girio, R. J. S.; Buchaim, D. V.; Bueno, P. C. D. S. The Effects of Curcumin on Diabetes Mellitus: A Systematic Review. *Front. Endocrinol. (Lausanne).* **2021**, *12*, 669448.
7. Quispe, C.; Herrera-Bravo, J.; Javed, Z.; Khan, K.; Raza, S.; Gulsunoglu-Konuskan, Z.; Daştan, S. D.; Sytar, O.; Martorell, M.; Sharifi-Rad, J.; Calina, D. Therapeutic Applications of Curcumin in Diabetes: A Review and Perspective. *BioMed. Res. Int.* **2022**, 1375892.
8. Bozkurt, O.; Kocaadam-Bozkurt, B.; Yildiran, H. Effects of curcumin, a bioactive component of turmeric, on type 2 diabetes mellitus and its complications: an updated review. *Food. Funct.* **2022**, *13*, 11999-12010.
9. Lu, W.; Shahidi, F. K.; Khorsandi, K.; Hosseinzadeh, R.; Gul, A.; Balick, V. An update on molecular mechanisms of curcumin effect on diabetes. J. *Food. Biochem*. **2022**, *46*, e14358.
10. Hodaei, H.; Adibian, M.; Nikpayam, O.; Hedayati, M.; Sohrab, G. The effect of curcumin supplementation on anthropometric indices, insulin resistance and oxidative stress in patients with type 2 diabetes: a randomized, double-blind clinical trial. *Diabetol. Metab. Syndr*. **2019**, *11*, 41.
11. Pivari, F.; Mingione, A.; Brasacchio, C.; Soldati, L. Curcumin and Type 2 Diabetes Mellitus: Prevention and Treatment. *Nutrients*. **2019**, *11*, 1837.
12. Roxo, D. F.; Arcaro, C. A.; Gutierres, V. O.; Costa, M. C.; Oliveira, J. O.; Lima, T. F. O.; Assis, R. P.; Brunetti, I. L.; Baviera, A. M. Curcumin combined with metformin decreases glycemia and dyslipidemia, and increases paraoxonase activity in diabetic rats. *Diabetol. Metab. Syndr*. **2019**, *11*, 33.
13. Rivera-Mancía, S.; Trujillo, J.; Chaverri, J. P. Utility of curcumin for the treatment of diabetes mellitus: Evidence from preclinical and clinical studies. *J. Nutr. Intermed. Metab*. **2018**, *14*, 29-41.
14. Wang, L.; Xu, J.; Yu, T.; Wang, H.; Cai, X.; Sun, H. Efficacy and safety of curcumin in diabetic retinopathy: A protocol for systematic review and meta-analysis. *PLoS. ONE*. **2023**, *18(4)*, e0282866.
15. Gupta, S. C.; Kismali, G.; Aggarwal, B. B. Curcumin, a component of turmeric: from farm to pharmacy. *Biofactors*. **2013**, *39*, 2-13.
16. Anand, P.; Kunnumakkara, A. B.; Newman, R. A.; Aggarwal, B. B. Bioavailability of curcumin: problems and promises. *Mol. Pharm.* **2007**, *4*, 807-818.
17. Naksuriya, O.; Okonogi, S.; Schiffelers, R. M.; Hennink, W. E. Curcumin nanoformulations: a review of pharmaceutical properties and preclinical studies and clinical data related to cancer treatment. *Biomaterials*. **2014**, *35*, 3365-3383.
18. Pourmadadi, M.; Abbasi, P.; Eshaghi, M. M.; Bakhshi, A.; Manicum, A. E.; Rahdar, A.; Pandey, S.; Jadoun, S.; Díez-Pascual, A. M. Curcumin delivery and co-delivery based on nanomaterials as an effective approach for cancer therapy. *J. Drug. Deliv. Sci. Technol.* **2022**, *78*, 103982.
19. Li, L.; Zhang, X.; Pi, C.; Yang, H.; Zheng, X.; Zhao, L.; Wei, Y. Review of Curcumin Physicochemical Targeting Delivery System. *Int. J. Nanomedicine*. **2020**, *15*, 9799–9821.
20. Zheng, B.; McClements, D. J. Formulation of More Efficacious Curcumin Delivery Systems Using Colloid Science: Enhanced Solubility, Stability, and Bioavailability. *Molecules*. **2020**, *25*, 2791.
21. Kesharwani, P.; Banerjee, S.; Padhye, S.; Sarkar, F. H.; Iyer, A. K. Hyaluronic Acid Engineered Nanomicelles Loaded with 3,4-Difluorobenzylidene Curcumin for Targeted Killing of CD44+ Stem-Like Pancreatic Cancer Cells. *Biomacromolecules*. **2015**, *16*, 3042–3053.
22. Datta, S.; Jutkova, A.; Šramkova, P.; Lenkavska, L.; Huntosova, V.; Chorva, D.; Miskovsky, P.; Jancura, D.; Kronek, J. Unravelling the Excellent Chemical Stability and Bioavailability of Solvent Responsive Curcumin-Loaded 2-Ethyl-2-oxazoline-grad-2-(4-dodecyloxyphenyl)-2-oxazoline Copolymer Nanoparticles for Drug Delivery. *Biomacromolecules*. **2018**, *19*, 2459−2471.
23. Zatorska-Plachta, M.; Lazarski, G.; Maziarz, U.; Forys, A.; Trzebicka, B.; Wnuk, D.; Choluj, K.; Karewicz, A.; Michalik, M.; Jamroz, D.; Kepczynski, M. Encapsulation of Curcumin in Polystyrene-Based Nanoparticles Drug Loading Capacity and Cytotoxicity. *ACS. Omega*. **2021**, *6*, 12168−12178.
24. Bagheri, M.; Fens, M. H.; Kleijn, T. G.; Capomaccio, R. B.; Mehn, D.; Krawczyk, P. M.; Scutigliani, E. M.; Gurinov, A.; Baldus, M.; Kronenburg, N. C. H. V.; Kok, R. J.; Heger, M.; Nostrum, C. F. V.; Hennink, W. E.

In Vitro and In Vivo Studies on HPMA-Based Polymeric Micelles Loaded with Curcumin. *Mol. Pharm*. **2021**, *18*, *3*, 1247–1263.

25. Obeid, M. A.; Alsaadi, M.; Aljabali, A. A. Recent updates in curcumin delivery. *J. Lipsome. Res*. **2023**, *33*, 53-64.
26. Feng, T.; Wei, Y.; Lee, R. J.; Zhao, L. Liposomal curcumin and its application in cancer. *Int. J. Nanomedicine*. **2017**, *12*, 6027-6044.
27. Lazar, A. N.; Mourtas, S.; Youssef, I.; Parizot, C.; Dauphin, A.; Delatour, B.; Antimisiaris, S. G.; Duyckaerts, C. Curcumin-conjugated nanoliposomes with high affinity for Ab deposits: possible applications to Alzheimer disease. *Nanomed*. **2013**, *9*, 712-721.
28. Mondal, G.; Barui, S.; Saha, S.; Chaudhuri, A. Tumor growth inhibition through targeting liposomally bound curcumin to tumor vasculature. *J. Control. Release.* **2013**, *172*, 832-840.
29. Arvapalli, D. M.; Sheardy, A. T.; Allado, K.; Chevva, H.; Yin, Z.; Wei, J. Design of Curcumin Loaded Carbon Nanodots Delivery System: Enhanced Bioavailability, Release Kinetics, and Anticancer Activity. *ACS. Appl. Bio. Mater.* **2020**, *3*, 8776–8785.
30. Mathew, M. S.; Vinod, K.; Jayaram, P. S.; Jayasree, R. S.; Joseph, K. Improved Bioavailability of Curcumin in Gliadin-Protected Gold Quantum Cluster for Targeted Delivery. *ACS. Omega.* **2019**, *4*, 14169−14178.
31. S, P. R.; Mal, A.; Valvi, S. K.; Srivastava, R.; De, A.; Bandyopadhyaya, R. Noninvasive Preclinical Evaluation of Targeted Nanoparticles for the Delivery of Curcumin in Treating Pancreatic Cancer. *ACS. Appl. Bio. Mater.* **2020**, *3*, 4643–4654.
32. Lawson, S.; Newport, K.; Pederniera, N.; Rownaghi, A. A.; Rezaei, F. Curcumin Delivery on Metal–Organic Frameworks: The Effect of the Metal Center on Pharmacokinetics within the M-MOF-74 Family. *ACS. Appl. Bio Mater.* **2021**, *4*, 3423–3432.
33. Kotcherlakota, R.; Barui, A. K.; Prashar, S.; Fajardo, M.; Briones, D.; Rodriguez-Dieguez, A.; Patra, C. R.; Gomez-Ruiz, S. Curcumin loaded mesoporous silica: an effective drug delivery system for cancer treatment. *Biomater. Sci.* **2016**, 4, 448-459.
34. Lin, Q.; Li, W.; Liu, D.; Zhao, M.; Zhu, X.; Li, W.; Wang, L.; Zheng, T.; Li, J. Porous Silicon Carrier Delivery System for Curcumin: Preparation, Characterization, and Cytotoxicity in Vitro. *ACS. Appl. Bio. Mater.* **2019**, *2*, 1041-1049.
35. Nasery, M. M.; Abadi, B.; Poormoghadam, D.; Zarrabi, A.; Keyhanvar, P.; Khanbabaei, H.; Ashrafizadeh, M.; Mohammadinejad, R.; Tavakol, S.; Sethi, G. Curcumin Delivery Mediated by Bio-Based Nanoparticles: A Review. *Molecules.* **2020**, *25*, 689.
36. Wang, L.; Li, J.; Xiong, Y.; Wu, Y.; Yang, F,; Guo, Y.; Chen, Z.; Gao, L.; Deng, W. Ultrashort Peptides and Hyaluronic Acid-Based Injectable Composite Hydrogels for Sustained Drug Release and Chronic Diabetic Wound Healing. *ACS. Appl. Mater. Interfaces.* **2021**, *13*, 58329–58339.
37. Gao, C.; Chu, X.; Gong, W.; Zheng, J.; Xie, X.; Wang, Y.; Yang, M.; Li, Z.; Gao, C.; Yang, Y. Neuron tau-targeting biomimetic nanoparticles for curcumin delivery to delay progression of Alzheimer's disease. *J. Nanobiotechnol.* **2020**, *18*, 71.
38. Yang, J.; Chen, X.; Wen, H.; Chen, Y.; Yu, Q.; Shen, M.; Xie, J. Curcumin-Loaded pH-Sensitive Biopolymer Hydrogels: Fabrication, Characterization, and Release Properties. *ACS. Food. Sci. Technol.* **2022**, *2,3*, 512-520.
39. Li, X.; He, Y.; Zhang, S.; Gu, Q.; McClements, D. J.; Chen, S.; Liu, X.; Liu, F. Lactoferrin-Based Ternary Composite Nanoparticles with Enhanced Dispersibility and Stability for Curcumin Delivery. *ACS. Appl. Mater. Interfaces.* **2023**, *15*, 18166-18181.
40. Wang, Z.; Zhang, R. X.; Zhang, C.; Dai, C.; Ju, X.; He, R. Fabrication of Stable and Self-Assembling Rapeseed Protein Nanogel for Hydrophobic Curcumin Delivery. *J. Agric. Food. Chem*. **2019**, *67*, 887−894.
41. Milenkova, S.; Manolov, I.; Pilicheva, B.; Nikolova, M.; Marudova, M. Curcumin loaded casein submicron-sized gels as drug delivery systems. *J. Phys. Conf. Ser.* **2021**, *1762*, 012009.
42. Reeves, A.; Vinogradov, S. V.; Morrissey, P.; Chernin, M.; Ahmed, M. M. Curcumin-encapsulating Nanogels as an Effective Anticancer Formulation for Intracellular Uptake. *Mol. Cell. Pharmacol.* **2015**, *7*, 25-40.
43. Bisht, S.; Mizuma, M.; Feldmann, G.; Ottenhof, N. A.; Hong, S.; Pramanik, D.; Chenna, V.; Karikari, C.; Sharma, R.; Goggins, M. G.; Rudek, M. A.; Ravi, R.; Maitra, A.; Maitra, A. Systemic administration of polymeric nanoparticle-encapsulated curcumin (NanoCurc™) blocks tumor growth and metastases in preclinical models of pancreatic cancer. *Mol. Cancer. Ther.* **2010**, *9*, 2255-2264.
44. Ray, B.; Bisht, S.; Maitra, A.; Maitra, A.; Lahiri D. K. Neuroprotective and Neurorescue Effects of a Novel Polymeric Nanoparticle Formulation of Curcumin (NanoCurc™) in the Neuronal Cell Culture and Animal Model: implications for Alzheimer's disease. *J. Alzheimers. Dis.* **2010**, *23*, 61-77.
45. Goncalves, C.; Pereira, P.; Schellenberg, P.; Coutinho, P. J.; Gama, F. M. Self-Assembled Dextrin Nanogel as Curcumin Delivery System. *J. Biomater. Nanobiotechnol.* **2012**, *3*, 178-184.
46. Luckanagul, J. A.; Pitakchatwong, C.; Bhuket, P. R. N.; Muangnoi, C.; Rojsitthisak, P.; Chirachanchai, S.; Wang, Q.; Rojsitthisak, P. Chitosan-based polymer hybrids for thermo-responsive nanogel delivery of curcumin. *Carbohydr. Polym.* **2018**, *181*, 1119-1127.

47. Dinari, A.; Abdollahi, M.; Sadeghizadeh, M. Design and fabrication of dual responsive lignin-based nanogel via "grafting from" atom transfer radical polymerization for curcumin loading and release. *Sci. Rep.* **2021**, *11*, 1962.
48. Santhamoorthy, M.; Kim, S. Dual pH- and Thermo-Sensitive Poly(N-Isopropylacrylamide-co-Allylamine) Nanogels for Curcumin Delivery: Swelling–Deswelling Behavior and Phase Transition Mechanism. *Gels*. **2023**, *9*, 536.
49. Howaili, F.; Özliseli, E.; Kucukturkmen, B.; Razavi, S. M.; Sadeghizadeh, M.; Rosenholm, J. M. Stimuli-Responsive, Plasmonic Nanogel for Dual Delivery of Curcumin and Photothermal Therapy for Cancer Treatment. *Front. Chem.* **2021**, *8*, 602941.
50. Oh, J. K.; Lee, D. I.; Park, J. M. Biopolymer-based microgels/nanogels for drug delivery applications. *Progress in Polymer Science.* **2009**, *34*, 1261–1282.
51. Yin, Y.; Hu, B.; Yuan, X.; Cai, L.; Gao, H.; Yang, Q. Nanogel: A Versatile Nano-Delivery System for Biomedical Applications. *Pharmaceutics.* **2020**, *12*, 290.
52. Preman, N. K.; Jain, S.; Johnson, R. P. "Smart" Polymer Nanogels as Pharmaceutical Carriers: A Versatile Platform for Programmed Delivery and Diagnostics. *ACS. Omega.* **2021**, *6*, 5075-5090.
53. Wu, W.; Shen, J.; Banerjee, P.; Zhou, S. Water-dispersible multifunctional hybrid nanogels for combined curcumin and photothermal therapy. *Biomaterials.* **2011**, *32*, 598-609.
54. Badi, N. Non-linear PEG-based thermoresponsive polymer systems. *Prog. Polym. Sci.* **2017**, *66*, 54-79.
55. Lutz, J. F.; Akdemir, Ö.; Hoth, A. Point by point comparison of two thermosensitive polymers exhibiting a similar LCST: is the age of poly(NIPAM) over. *J. Am. Chem. Soc.* **2006**, *128*, 13046-7.
56. Liu, M.; Leroux, J. C.; Gauthier M. A. Conformation-function relationships for the comb-shaped polymer pOEGMA. *Prog. Polym. Sci.* **2015**, *48*, 111-121.
57. Lutz, J. F. Polymerization of oligo(ethylene glycol) (meth)acrylates: toward new generations of smart biocompatible materials. *J. Polym. Sci. Part. A. Polym. Chem.* **2008**, *46*, 3459-3470.
58. Hu, Z.; Cai, T.; Chi, C. Thermoresponsive oligo(ethylene glycol)-methacrylatebased polymers and microgels. *Soft Matter.* **2010**, *6*, 2115-2123.
59. Lutz, J. F. Thermo-switchable materials prepared using the OEGMA-platform. *Adv. Mater.* **2011**, *23*, 2237-2243.
60. Ghosh, S.; GhoshMitra, S.; Cai, T.; Diercks, D. R.; Mills, N. C.; Hynds, D. A. L. Alternating Magnetic Field Controlled, Multifunctional Nano-Reservoirs: Intracellular Uptake and Improved Biocompatibility. *Nanoscale. Res. Lett.* **2010**, *5*, 195.
61. Hayes, J. L.; Ingram, L. L.; Strom, L. B.; Roton, L. M.; Boyette, M. W.; Walsh, M. T. In Vozzo, J. A. ed. Proceedings of the 4th Southern Station Chemical Sciences Meeting. *USDA Forest Service, Southern Forest Experiment Station, General Technical Report SO-104*. **2004**, 69-80.
62. Fiege, H.; Voges, H. W.; Hamamoto, T.; Umemura, S.; Iwata, T.; Miki, H.; Fujita, Y.; Buysch, H. J.; Garbe, D.; Paulus, W. "Phenol Derivatives" in Ullmann's Encyclopedia of Industrial Chemistry. *Wiley-VCH. Weinheim.* **2002**, 521-582.
63. Chi, C.; Cai, T.; Hu, Z. Oligo(ethylene glycol)-Based Thermoresponsive Core–Shell Microgels. *Langmuir.* **2009**, *25*, 3814-3819.
64. Schneider, C.; Gordon, O. N.; Edwards, R. L.; Luis, P. B. Degradation of curcumin: From mechanism to biological implications. *J. Agric. Food. Chem.* **2015**, *63*, 7606-7614.
65. Wang, Y.; Pan, M..; Cheng, A..; Lin, L.; Ho, Y..; Hsieh, C.; Lin, J. Stability of curcumin in buffer solutions and characterization of its degradation products. *J. Pharm. Biomed. Anal.* **1997**, *15*, 1867-1876.
66. Mondal, S.; Ghosh, S.; Moulik, S. P. Stability of curcumin in different solvent and solution media: UV–visible and steady-state fluorescence spectral study. *J. Photochem. Photobiol. B*. **2016**, *158*, 212-218.